# Discontinuous bundling transition in semiflexible polymer networks induced by Casimir interactions

Devin Kachan, Kei W. Müller, Wolfgang A. Wall, and Alex J. Levine

Phys. Rev. E **94**, 032505 — Published 19 September 2016

DOI: 10.1103/PhysRevE.94.032505

# Discontinuous bundling transition in semiflexible polymer networks induced by Casimir interactions

Devin Kachan[1], Kei W. Müller[2], Wolfgang A. Wall[2], and Alex J. Levine[1,3,4]
[1]*Department of Physics, UCLA, Los Angeles, CA 90095-1596*
[2]*Institute for Computational Mechanics, Technische Universität München, 85748 Garching, Germany*
[3]*Department of Chemistry & Biochemistry and*
[4]*The California Nanosystems Institute, UCLA, Los Angeles, CA 90095-1596*
(Dated: August 26, 2016)

Fluctuation-induced interactions are an important organizing principle in a variety of soft matter systems. We investigate the role of fluctuation-based or thermal Casimir interactions between cross linkers in a semiflexible network. One finds that, by integrating out the polymer degrees of freedom, there is an attractive logarithmic potential between nearest neighbor cross linkers in a bundle, with a significantly weaker next-nearest-neighbor interaction. Here we show that a one-dimensional gas of these strongly interacting linkers in equilibrium with a source of unbound ones admits a discontinuous phase transition between a sparsely and a densely bound bundle. This discontinuous transition induced by the long-ranged nature of the Casimir interaction allows for a similarly abrupt structural transition in semiflexible filament networks between a low cross linker density isotropic phase and a higher cross link density bundle network. We support these calculations with the results of finite element Brownian dynamics simulations of semiflexible filaments and transient cross linkers.

PACS numbers: 87.16.Ka,05.40.-a,82.35.Lr

## I. INTRODUCTION

Semiflexible networks with transient cross linkers form the main structural elements of the cytoskeleton of eukaryotic cells, and provide an intriguing arena in which to study nonequilibrium physics. Due to the steric interactions between the long filaments (e.g. F-actin) these systems are typically frustrated, unable to reach more ordered ground states [1]. In spite of this steric frustration, experiments [2–6] have found that both the statistical properties of the network's structure and its mechanics (rheology) can be reproducibly predicted as a function of the ratio of the concentrations of the filaments and their cross linkers. In particular, one observes an abrupt transition between networks composed of filaments and networks composed of filament bundles as a function of cross linker concentration and species. This seems surprising as one might expect there to be continuous growth of bundles with increasing cross linker density, cutoff in the high cross linker limit only by the aforementioned steric frustration.

In this article we propose that one can understand the abruptness of the bundling transition in semiflexible networks by considering the Casimir or fluctuation-based interaction between cross linkers bound to the same filament. The basic physics of this Casimir interaction in semiflexible polymers has been explored previously [7]. It produces a long-ranged attractive interaction between neighboring cross linkers owing to their modification of the small (tens of nanometers) transverse undulations of the filaments. We present new calculations showing that, due to the long-range nature of the Casimir interaction, there is an abrupt condensation transition in which a gas of free cross linkers abruptly lock nearly parallel filaments into bundles as a function of cross linker concentration. We also test the predictions of the fundamental Casimir interaction between cross linkers and the condensation transition based on this interaction using large-scale Brownian dynamics finite-element simulations of the network.

This first order condensation transition appears in spite of the one-dimensional nature of the problem due to the long-range (logarithmic) nature of the fluctuation-induced interaction between cross linkers (violating the van Hove condition [8]). This allows for the abrupt condensation transition in the line density of cross linkers on the filament at a critical value of their chemical potential. In the condensed phase one finds that the bound-linker line density is significantly enhanced relative to that expected from a simple Langmuir isotherm [9]. In fact, one rapidly reaches bound-linker saturation, where their line density is limited only by their hardcore repulsion. Below the condensation point, one finds large linker density fluctuations, but a small mean concentration, implying insignificant bundling. Thus, we find that Casimir interactions between linkers produce a type of binary chemical switch controlled by linker concentration between two states: (i) free filaments and a solution of unbound cross linkers below the transition, and (ii) bundles composed of filaments that are maximally coated with cross linkers. We also show that the existence of the first order bundling transition depends on the type of cross linker. Specifically, only cross linkers of the "bundling type," i.e., those that constrain the local angle between filaments at the cross link, are capable of inducing an abrupt, first-order bundling transition.

The article is organized as follows: Section II briefly reviews the pairwise Casimir interaction between cross linkers on a semiflexible filament. Section III presents evidence from Brownian dynamics finite element simu-

lations for the existence of the interaction in physical systems. In sections IV and V we introduce theoretical and simulation results, respectively, showing that the interaction leads to a sharp condensation transition in solutions of cross linkers that constrain the angle between the two bound filaments. These "bundling" cross linkers admit a first order bundling transition at a critical linker concentration. That transition changes the character of the network from a network of individual filaments to a network of their bundles. We briefly summarize and comment on the broader biophysical implications of this result in section VI.

## II. CASIMIR INTERACTIONS

The deformations h(z) of a fluctuating semiflexible filament of length $L$ with bending modulus $\kappa$ at temperature $T$ can be described in cases where the filament is much shorter than its thermal persistence length, $L \ll \kappa/T$, (setting Boltzmann's constant $k_B = 1$) by the quadratic Hamiltonian

$$\mathcal{H} = \frac{\kappa}{2}\int_0^L \mathrm{dz}\ [\partial_z \mathrm{h(z)}]^2 \,. \tag{1}$$

We assume zero applied tension and that the undeformed filament is directed along the $z$ axis – see Fig. 1(C). If cross linkers then bind to this filament such that they pin its position (e.g., against an elastic background of other filaments – see Fig. 1(A) ), these cross linkers *reduce* the filament's entropy. This effect leads to a logarithmic Casimir [10] interaction between consecutive cross linkers bound to the same filament and separated by a distance $x$:

$$V(x) = d_\perp \alpha T \log\left(\frac{x}{\lambda_c}\right). \tag{2}$$

Here $d_\perp$ is the number of transverse fluctuation dimensions and $\alpha$ counts the number of degrees of freedom pinned by a cross linker. For example, if the cross linker exerts only constraint forces to pin the filament's position, $\alpha = 1$ (e.g., "network" cross linkers such as filamin [11]), but if the cross linkers also produce constraint torques to control the angle between the crossing filaments, $\alpha = 2$ (e.g., "bundling" cross linkers such as $\alpha$-actinin or fascin [11]). Soft constraints, such as those produced if the linkers were to introduce a harmonic potential controlling these degrees of freedom result in intermediate values of $\alpha$. The length $\lambda_c$ represents the volume of phase space of a single filament state and is related to $\hbar$ – see Ref. [7] for details.

The logarithmic form of the Casimir interaction has a superficial resemblance to the loop entropy of *flexible* polymers [12], but has a different origin [7]. The Casimir interaction differs in at least two specific ways from the loop entropy contribution to the free energy of a flexible polymer loop. First, the Casimir potential as calculated

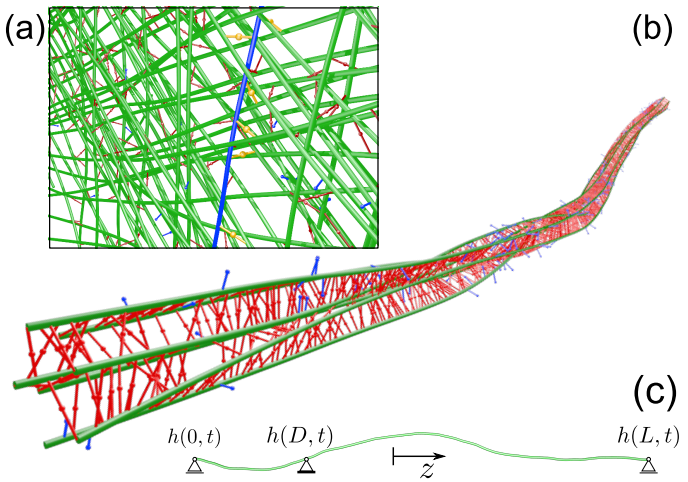


FIG. 1: (color online) (a) A typical realization of a semiflexible gel. The fluctuations of a given filament (blue) are reduced by the cross linking (orange linkers) between it and the network, which is itself a cross linked gel (red linkers). (b) Finite element simulation of bundle formation via the Casimir-induced linker condensation: doubly (singly) bound linkers shown in red (blue). (c) Finite element-based test of Casimir interactions between three linkers (triangles) on one filament.

applies only to cases where the filament is shorter than its own persistence length, where the standard calculation of the logarithmic loop entropy is inapplicable. Second and most importantly the dependence of the potential on the (chemical) details of the cross linker through the parameter $\alpha$ emerge only through the Casimir interaction on semiflexible filaments. The loop entropy of flexible polymers admits no such effect. By treating the polymer as flexible, loop entropy cannot depend on the details of how the cross linker constrains either the direction of the local tangent or, in fact, higher derivatives. Such constraints affect the entropy of only one persistence length of the flexible chain, which constitutes a negligible correction in that case. The effect of the Casimir interactions in cross linked stiff filaments will be shown to depend critically upon the type of cross linker, parameterized by the $\alpha$ in Eq. 2. Due to the fact that both the filament and the distance between consecutive cross linkers are small compared to the persistence length, the constraint on the local filament tangent (and in principle, higher derivatives than the tangent) may propagate across the entire system and thereby have substantial effects. We will see that the first-order bundling transition occurs only above a critical value of $\alpha$.

## III. SIMULATION OF THE FUNDAMENTAL CASIMIR INTERACTION

To test the effective potential induced between two cross linkers by the Casimir interaction, we performed a

Brownian dynamics finite element simulation of a semi-flexible filament with fixed cross linkers. Our computational approach [13, 14] models single filaments with geometrically exact, nonlinear Timoshenko beam elements [15–17], which account for axial, torsional, bending, and shear deformation. Viscous drag forces at the element level are modeled by

$$\boldsymbol{f}_{visc} = \boldsymbol{c}_t \dot{\boldsymbol{x}}, \qquad \boldsymbol{m}_{visc} = \boldsymbol{c}_r \dot{\boldsymbol{\theta}}, \tag{3}$$

with translational and rotational damping tensors

$$\mathbf{c}_t = \begin{bmatrix} \gamma_{\parallel} & 0 & 0 \\ 0 & \gamma_{\perp} & 0 \\ 0 & 0 & \gamma_{\perp} \end{bmatrix}, \quad \mathbf{c}_r = \begin{bmatrix} \gamma_a & 0 & 0 \\ 0 & 0 & 0 \\ 0 & 0 & 0 \end{bmatrix}, \tag{4}$$

which are given in local coordinates, and translational and rotational velocities $\dot{\boldsymbol{x}}$ and $\dot{\boldsymbol{\theta}}$. Since the filament length $L$ is far below the persistence length, hydrodynamic damping constants $\zeta_{(.)}{=}\gamma_{(.)}L$ for straight rigid cylinders can be taken from the literature [18]. Stochastic forces and moments are determined in accordance to the fluctuation-dissipation theorem

$$\begin{aligned} \boldsymbol{f}_{stoch} &= \sqrt{2T}\boldsymbol{s}_t \frac{\partial \boldsymbol{\mathcal{W}}_t^2(s,t)}{\partial s \partial t} \\ \boldsymbol{m}_{stoch} &= \sqrt{2T}\boldsymbol{s}_r \frac{\partial \boldsymbol{\mathcal{W}}_r^2(s,t)}{\partial s \partial t}, \end{aligned} \tag{5}$$

where the damping tensors $\boldsymbol{s}_{\{t,r\}}$ are chosen to satisfy $\boldsymbol{s}_{\{t,r\}}{\boldsymbol{s}_{\{t,r\}}}^T = \boldsymbol{c}_{\{t,r\}}$, and $\boldsymbol{\mathcal{W}}$ denotes a standard Wiener process.

Time is discretized using an *Implicit-Euler* scheme, which, due to better numerical stability, allows for larger step sizes and therefore much greater simulated time intervals as compared to explicit schemes. Full details on the mechanical model, the numerical method and the discretization in time are given in Ref. [13, 19, 20].

The simulation studied a single filament of length $L = 10\mu$m and persistence length $L_p \approx 18.4\mu$m, discretized with $N = 4000$ beam finite elements, constituting 24000 degrees of freedom. Its circular cross section area was set to $A = 1.9{\times}10^{-5}\mu\text{m}^2$ leading to a high axial stiffness compared to its bending stiffness. The moment of inertia of area is set to $I = 2.85{\times}10^{-11}\mu\text{m}^4$ and the polar moment of inertia to $I_p = 5.7{\times}10^{-11}\mu\text{m}^4$. The initial, stress-free geometry was chosen straight and parallel to the global $z$-direction. Its movement was constrained to two dimensions, allowing for a single dimension of transverse deflections of the filament. Temperature was set to $T = 293$K and the dynamic viscosity of the fluid to $\eta = 10^{-3}$ Pa s.

Three different step sizes $\Delta t \in \{10^{-2}\text{s}; 10^{-4}\text{s}; 10^{-6}\text{s}\}$ of the time integration scheme were chosen in order to access a broad set of geometrical configurations of the filament: A large $\Delta t$ allows for efficient sampling of low frequency modes, while a small $\Delta t$ is needed to sample the high frequency modes. Fig. 2, which compares the observed Fourier displacement mode amplitudes $A_n$ for a filament with hinged boundary conditions at the endpoints to the expected result from equipartition, $A_n^2 = T/\kappa k_n^4$ for modes with wavenumber $k_n = n\pi/L$, shows that the three time steps chosen collectively allow for accurate sampling of approximately the first 30 harmonic modes. All cases were simulated for $> 2 \times 10^5$ time steps.

A cross link along the filament was implemented by pinning the displacement at that point while leaving the filament free to rotate ($\alpha = 1$). This is equivalent to assuming both the cross linkers and background network, shown in Fig. 1(A), are perfectly incompliant. Relaxing this requirement introduces a local harmonic potential at the pinning site, but does not qualitatively change the Casimir interaction [7]. The ends of the filament were similarly fixed by the same hinged boundary conditions – see Fig. 1(C). To maintain a tension-free filament, the ends were allowed to move freely in the longitudinal ($\hat{z}$) direction.

The potential Eq. 2 is difficult to directly measure because it represents a free energy change $\sim T$ between two differing linker configurations, each of which has free energies on the scale of $NT$, where $N$ is the macroscopic number of filament degrees of freedom. Fortunately, the Casimir interaction generates a linear coupling between Fourier modes of the filament's deformation so that the linker's effect on the free energy may be directly observed from the covariance matrix of these Fourier amplitudes $A_n$, $n = 0, 1, 2, \ldots$, of filament displacement. Specifically, we place one linker at $z = D$ and measure directly the changes in the amplitude correlation functions $\langle A_n A_m \rangle$ that result. Based on the above model, these correlations take the form

$$\langle A_i A_j \rangle = \frac{T}{\kappa} \left[ \frac{\delta_{ij}}{k_i^4} - \frac{\frac{\sin k_i D}{k_i^4} \frac{\sin k_j D}{k_j^4}}{\sum_{n=1}^{N} \frac{\sin^2 k_n D}{k_n^4}} \right], \tag{6}$$

for modes with wavenumber $k_n = n\pi/L$. The first term gives the standard equipartition result for the filament with hinged ends only; the effect of the linker at $0 < D < L$ modifies this result bringing in off-diagonal corrections. The numerically obtained covariance matrices are well fitted by Eq. 6 as shown in Fig. 3 for a representative example with $\alpha = 1$. Errors are generally on the order of 10% and decrease with additional observations.

## IV. DISCONTINUOUS BUNDLING TRANSITION

The extension of the two-particle Casimir interaction to a large number of cross linkers in a network has two nontrivial features: (i) Because cross linkers will only interact if they are on the same filament, the full interaction energy of a network configuration depends explicitly on the network topology, and (ii) a single filament's degrees of freedom on either side of the cross linker are coupled by the condition of slope continuity, leading to an interaction which is not strictly nearest-neighbor. For

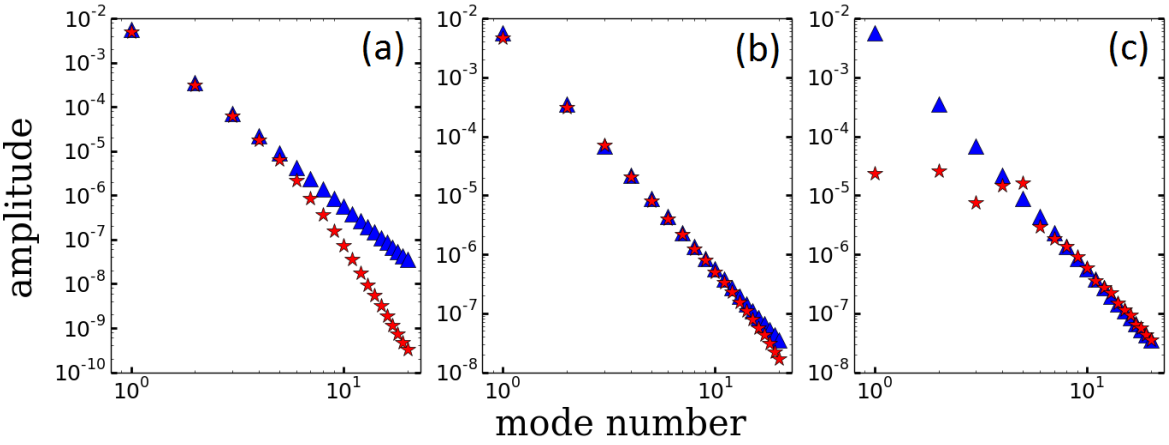


FIG. 2: (color online) Comparison of theoretical (▲) Fourier displacement mode amplitudes for a filament hinged at both ends to those computed (★) from finite element simulations for time discretizations $\Delta t = 10^{-2}$s, $10^{-4}$s, and $10^{-6}$s, shown in (a), (b), and (c), respectively. Large (small) time steps are necessary to sample slow (fast) modes, and collectively the chosen time steps allow one to accurately examine the first 30 modes.

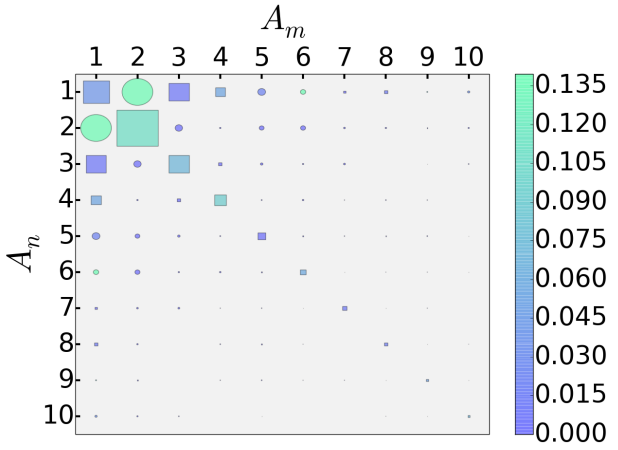


FIG. 3: (color online) The Fourier amplitude covariance matrix $\langle A_n A_m \rangle$ for the first 10 displacement modes $A_n$ from simulation of a filament pinned at $D = 0.4L$. The area and shape of each element represents its log-normalized magnitude and sign (square + vs. circle −) respectively. The color bar indicates the % error relative to Eq. 6. The error magnitude is consistent across different pinning locations.

these reasons, a treatment of general networks is difficult, but one particularly simple topology, the *bundle*, is amenable to analytic calculations. Moreover bundling cross linkers, which necessarily require the slope to vanish by quenching angular fluctuations, generate a strictly nearest-neighbor interaction since the fluctuations on either side of the cross linker are decoupled.

The simplest bundle model, which we consider here, consists of two parallel filaments sufficiently close together so that linkers may join them. We assume that each bundling linker quenches $\alpha$ local degrees of freedom on the filaments (e.g., $\alpha = 2$ implies that the linker pins both the position and slope of the filaments) leading to a Casimir interaction (given by Eq. 2) between nearest-neighbors only. The vanishing of second- and higher-nearest-neighbor interactions is valid for $\alpha \geq 2$; we expect only a weak second nearest-neighbor interaction for $1 \leq \alpha < 2$ [28]. The $x = 0$ singularity of the potential is cut off by the hard core repulsion of the linker with radius $a/2$ so that the linker potential becomes

$$V(x) = \begin{cases} \infty & x < a \\ d_\perp \alpha T \log\left(\frac{x}{\lambda_c}\right) & x > a \end{cases} \tag{7}$$

The equation of state of linkers in the grand canonical ensemble interacting via the hard core repulsion and logarithmic Casimir attraction can be solved exactly in the thermodynamic limit of infinite length filaments using standard techniques [21]. We begin with the partition sum of linkers in the bundle interacting with nearest neighbor potential $V(x)$ written as an integral over the positions $x_i$, $i = 1, \ldots N$ of the linkers. The contribution of the configurational degrees of freedom for this one dimensional system of size $L$ is given by

$$\begin{aligned} Z_N(L) \;=\; & \int\cdots\int_{0<x_1<x_2<\cdots<x_N<L} \mathrm{d}x_1 \cdots \mathrm{d}x_N \exp\left\{-\frac{1}{T}\left[V(x_1)\right.\right. \\ & + \left.\left. V(x_2 - x_1) + \cdots + V(L - X_N)\right]\right\}, \end{aligned} \tag{8}$$

where we have assumed that the particle-wall interaction is equivalent to the particle-particle interaction. The momentum degrees of freedom, which are decoupled from the configurational integrals and yield a product of thermal de Broglie wavelengths, are presently neglected but will be reinstated at the end of the calculation. Because Eq. 8 has the form of an $N$ fold convolution of the function

$$\Omega(R) = e^{-\frac{V(R)}{T}}, \tag{9}$$

the partition function may be written succinctly as

$$Z_N(L) = \underbrace{\Omega \star \Omega \star \cdots \star \Omega}_{N}. \tag{10}$$

Using the fact that convolutions map onto multiplication in Laplace space, the Laplace transform of the configurational integral is given by

$$\begin{aligned} Z_N(s) &= [\Omega(s)]^N \\ \Omega(s) &= \int_0^\infty e^{-sx - \frac{V(x)}{T}}\, \mathrm{dx}. \end{aligned} \tag{11}$$

Additionally, we have from the definition of $Z_N(s)$

$$\begin{aligned} Z_N(s) &= \int_0^\infty \mathrm{d}L\, Z_N(L) \exp\{-sL\} \\ &= \int_0^\infty \mathrm{d}L \exp\left\{-\frac{1}{T}(F + sTL)\right\}, \end{aligned} \tag{12}$$

where $F$ is the configurational part of the Helmholtz free energy, $F = -T \log Z$. In the large $N$ limit, the integral is expected to be sharply peaked so we may safely replace the integral by its largest value,

$$Z_N(s) \approx \exp\left\{-\frac{1}{T}(F + sTL)\right\}. \tag{13}$$

The extremal condition requires

$$\frac{\mathrm{d}}{\mathrm{dL}}(F + sTL) = 0, \tag{14}$$

implying that the quantity $p \equiv sT = -\frac{\mathrm{dF}}{\mathrm{dL}}$, should be interpreted as the pressure of the system.

With this association, we recognize $F + sTL = F + pL$ as the configurational contribution to the Gibbs free energy $G$. Furthermore, for an extensive system (appropriate for strictly nearest neighbor interactions) $G = \mu N$, where $\mu$ is the chemical potential. Comparing with the direct evaluation of the partition function Eq. 11 one finds

$$Z_N(s) = \exp^{-\frac{\mu}{T}N} = \left[\int_0^\infty e^{-\frac{px + V(x)}{T}}\, \mathrm{dx}\right]^N. \tag{15}$$

The result is an implicit relation between the pressure $p(T, \mu)$, which has units of force in one dimension, of the linkers in the bundle, temperature, and their chemical potential $\mu$. Substituting the pairwise, hard-core, Casimir-linker potential Eq. 7 for $V(x)$, and including the contribution of the kinetic degrees of freedom, one finds the equation of state

$$\mu = -T \log\left[\frac{T}{\lambda_t p}\left(\frac{\lambda_c p}{T}\right)^{d_\perp \alpha} \Gamma\left(1 - d_\perp\alpha, \frac{pa}{T}\right)\right], \tag{16}$$

where $\lambda_t$ is the thermal de Broglie wavelength, and $\Gamma(s, x)$ is the upper incomplete gamma function.

The chemical potential of the linkers on the bundle may be controlled by allowing them to come into chemical equilibrium with a solution of free linkers at number density $c$; treating the linker solution as an ideal gas, one finds $\mu = T \log c\lambda_t^d$. Deviations from ideality in the solution phase may be accounted via standard methods but are immaterial to our discussion.

The line density $\rho \equiv \frac{Na}{L}$, which is obtained by differentiating Eq. 16 with respect to $\mu$, defines the analog of the Langmuir isotherm [9] for the system. It reads

$$\rho = a\frac{\partial p}{\partial \mu} = \frac{pa}{T}\frac{\Gamma\left(1 - d_\perp\alpha, \frac{pa}{T}\right)}{\Gamma\left(2 - d_\perp\alpha, \frac{pa}{T}\right)}, \tag{17}$$

where the pressure is given implicitly through Eq. 16. The $\alpha = 0$ limit reproduces the Langmuir adsorption isotherms for linkers treated as an ideal gas with finite hard core volumes – a Tonks gas [22] – see Fig. 6.

For $\alpha > 0$ the long-range nature of the Casimir interaction leads to a remarkable result in infinitely long bundles: for sufficiently strong linker interactions $d_\perp\alpha > 1$, their density in the bundle vanishes when the linker chemical potential falls below the critical value $\mu \leq \mu_{\mathrm{crit}} = T \log[\frac{\lambda_c}{\lambda_t}(d_\perp\alpha - 1)]$. Moreover, for $d_\perp\alpha > 2$, upon increasing $\mu$ past $\mu_{\mathrm{crit}}$, the line density jumps discontinuously from 0 to $\rho = \rho_{crit} = \frac{d_\perp\alpha - 2}{d_\perp\alpha - 1}$. Due to the Casimir interaction, this condensed linker phase is actually a highly correlated fluid, even at low densities [23].

Both of these results persist in finite-length bundles, as confirmed both analytically by introducing a long distance cutoff to the interaction and computationally via Monte Carlo simulations of $N = 10000$ particles adsorbing onto a line at fixed chemical potential with Metropolis-Hastings dynamics. A comparison of the Monte Carlo results (points) and the analytic calculations (lines) for infinite length filaments are shown in Figs. 4 and 5. In Fig. 4, we observe that the one-dimensional pressure of the linkers at fixed line density actually vanishes below a critical concentration owing to the Casimir interaction canceling the entropic (essentially, ideal gas) pressure of the hard-core linker fluid. When the linkers in the filament bundle are in chemical equilibrium with a linker reservoir at fixed chemical potential (e.g., solution of linkers), we observe the expected jump in bound linker density at a critical chemical potential: $c_{\mathrm{crit}} : \mu(c_{\mathrm{crit}}) = \mu_{\mathrm{crit}}$. This linker condensation transition is somewhat rounded for finite-length filaments but remains remarkably sharp in comparison to the Langmuir isotherm of a simple Tonks gas, a system with hard core repulsion but no long-range Casimir interaction.

We note that a similar transition occurs for linkers that restrict the torsional fluctuations of a bundle [24]. Furthermore, we note that any generic logarithmic inter-linker potential will induce a similar transition. For example, flexible polymer bundles, which have an effective logarithmic inter-linker interaction due to the loop entropy of the polymers, have been shown to display condensation behavior [25, 26]. The Casimir interaction,

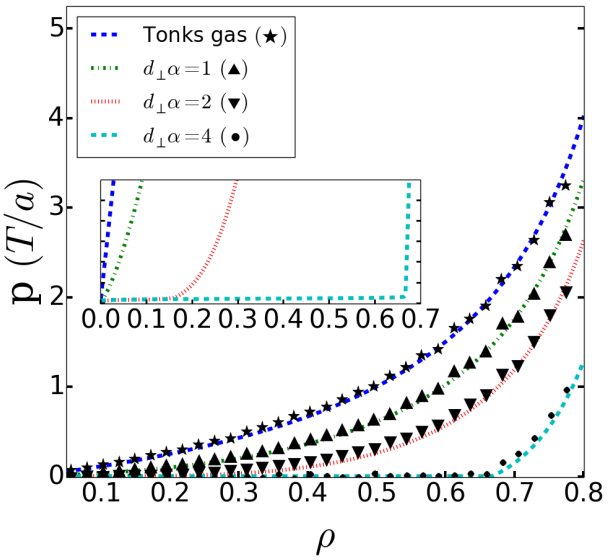


FIG. 4: (color online) The equation of state of the 1D Casimir gas for different values of the interaction strength $d_\perp\alpha$. The dashed lines representing solutions to Eq. 17 agree with Monte Carlo simulations (points). At high densities, the hard-core repulsion dominates forcing the equation of state to approach that of the Tonk's gas. INSET: The Casimir interaction dramatically reduces the pressure at low densities. For $d_\perp\alpha > 2$ it vanishes for $\rho < \rho_{\rm crit}$.

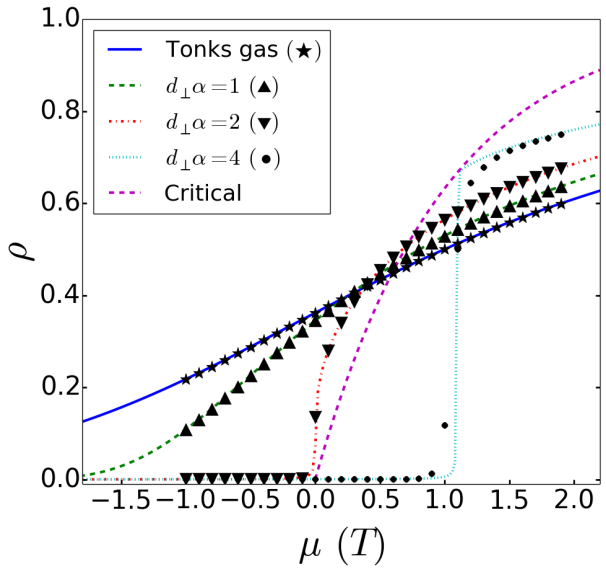


FIG. 5: (color online) Langmuir isotherms of a Casimir gas in equilibrium with an ideal gas of cross linkers at fixed chemical potential. The points represent results from grand canonical Monte Carlo simulations of $N = 10000$ particles adsorbing onto a line and interacting with the hard core Casimir potential. For $d_\perp\alpha > 2$ the system undergoes a condensation transition in the thermodynamic limit: The cross linkers spontaneously condense to the critical density $\rho_{\rm crit} = \frac{d_\perp\alpha-2}{d_\perp\alpha-1}$ at $\mu_{\rm crit} = k_{\rm B}T \log\left[\frac{\lambda_c}{\lambda_t}(d_\perp\alpha - 1)\right]$. Note the softening of the transition for $d_\perp\alpha = 4$ due to finite size effects.

however, should be the dominant mechanism for inducing bundling in biopolymer filaments, where the linker spacing is always well below the persistence length of the filaments.

At small chemical potential $\mu$, the decrease in linker density in the bundle with increasing $\alpha$ is surprising, given the attractive nature of the Casimir interaction. At low density, however, adding another linker to the bundle introduces an entropic contribution to the free energy $\sim -T \log L/N$ but this can be more than offset by the loss in filament entropy, which is the source of the Casimir interaction, $\sim d_\perp\alpha T \log L/N$, leading to a net increase in free energy due to the additional linker. This is possible because both the translational entropy of the linker and its Casimir interactions are entropic and thus proportional to $T$.

## V. SIMULATION OF THE BUNDLING TRANSITION

We turn to large-scale, finite-element, Brownian dynamics simulations to explore the effect of Casimir interactions in larger and more complex bundles, such as those expected in cytoskeletal networks. The computational methods are the same as those used in the numerical studies already discussed in Sec. III. Here we used those methods to simulate a single central filament surrounded by six outer filaments, all subject to hinged boundary conditions at one end – see Fig. 1(B). This configuration avoids the potential for frustrated dynamics associated with bundle formation, and is large enough to allow for multiple filament interactions within the bundle, while remaining computationally tractable. We expect that larger bundles of filaments should behave in similar ways, but may trap more filament twists, which then relax on very long time scales. We discuss this point further in the summary. The seven filament bundle was immersed in a solution of cross linkers that pin the slope of the filaments ($\alpha = 2$) at fixed concentration (therefore fixed chemical potential). The filaments were allowed to move in three dimensions ($d_\perp = 2$) (subject to their fixed boundary conditions at one end), so the expected prefactor in the Casimir potential is $d_\perp\alpha = 4$. Thus, we expect to observe a first-order bundling transition at a critical chemical potential of the cross linkers.

The Langmuir isotherms for simulations of two different length bundles are shown in Fig. 6 alongside a best theoretical fit (dot-dashed, green line) with two free parameters: a trivial horizontal shift representing a choice of reference chemical potential, and a vertical scaling which effectively tunes the strength of the hard-core repulsion. For comparison, we also plot the best fit Lang-

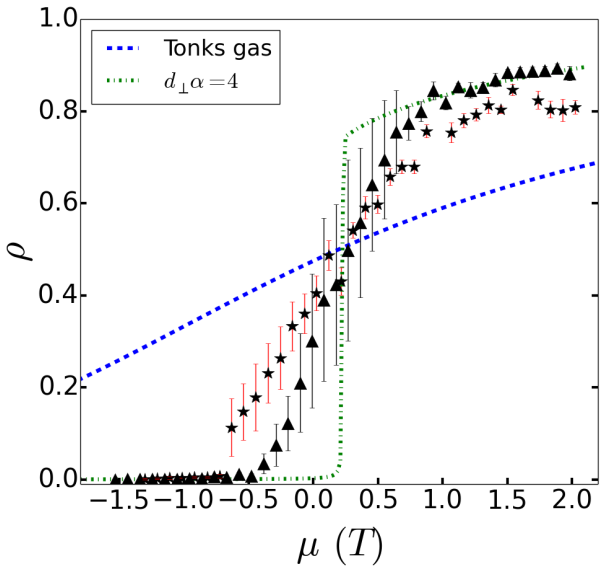


FIG. 6: (color online) Theoretical and simulated Langmuir isotherms of linkers adsorbed onto a filament bundle. (★) Simulation data for a 5$\mu$m bundle with persistence length $l_p = 9.2\mu$m. (▲) Both the system size and the persistence length doubled to study finite size scaling effects. The transition is noticeable sharper and is approaching the expected thermodynamic limit.

muir isotherm for a Tonks gas (dashed, blue line), showing that, without the Casimir interaction, one cannot account for the sharpness of the condensation transition. As the bundles are made longer (filled triangles) the transition is observed to become even sharper in the simulation, suggesting that the observed rounding is a finite size effect.

The large error bars near the transition indicate significant density fluctuations. These may be understood by inverting Eq. 17 to give the pressure in terms of of density, as shown in Fig. 4. Bound linker number fluctuations $\langle(\Delta N)^2\rangle/N^2$ are proportional to $\left(\frac{\partial p}{\partial L}\right)^{-1} = -L^2N^{-1}\left(\frac{\partial p}{\partial \rho}\right)^{-1}$. For $d_\perp\alpha > 1$, the derivative of the pressure with respect to density vanishes at small densities resulting in large density fluctuations.

## VI. CONCLUSIONS

We have demonstrated the predicted Casimir interactions between cross linkers in semiflexible filament networks in large scale numerical simulations. Using the previously obtained effective Casimir potential between consecutive cross linkers, now validated numerically, we predict a type of first-order bundling transition in which at a critical linker concentration, a network should transition from individual filaments to bundles. This abrupt transition (which is actually discontinuous in the thermodynamic limit) is quite distinct from the naive Langmuir adsorption behavior of sticky linkers binding to a filament network. The abruptness of this transition suggests that, due to strong collective effects, the chemical system of semiflexible filaments and bundling cross linkers admits a type of binary switch between two different morphologies, controlled by the concentration of the linkers.

Cells may take advantage of *equilibrium* Casimir interactions to control cytoskeletal structure. They might exploit this strongly interacting system to effect dramatic topological rearrangements of the cytoskeleton via small changes in the concentration of cross linking proteins, by tuning the linker concentration to near the critical one. As such they might capitalize on this high susceptibility point where small changes in protein expression levels lead to large scale network rearrangements. The difference in the elastic response of filament networks and bundle networks is stark [27], and potentially amenable to precise chemical control, at least for linker chemical potential near $\mu_{\rm crit}$. Alternatively, cells may tune linker concentrations far from this high susceptibility point in order to effectively decouple linker concentration from their cytoskeletal structure.

We also note from our simulations that upon the addition of linkers to a previously oriented set of filaments, the resulting bundle contains a number of quenched in twists. The bundle takes the form of a random braid. An example of such a twist is seen in Fig. 1B, where a complex twist of multiple filaments is seen in the middle of structure. Over the course of our simulations we did not observe the subsequent relaxation of these twisted structures. We expect that the expulsion of twist from the bundle is quite likely to be a slow process in that many linkers must be broken to eliminate a twist from the middle of the bundle. As a result, we expect that twist relaxation results from the slow process of twist diffusion to the ends of the bundle.

The broadest extension of the present work is addressing the analog of this bundling transition in a complex filament *network*. Since linkers interact only when bound to the same filaments, their Casimir interactions are both long-ranged and highly selective, acting over long distances in the network but only along select pathways. As such, the Casimir interactions both control and depend on the evolving network topology. For example, one may ask whether the linker gas could drive the alignment of parallel filaments in a bundle in order to maximize the length over which doubly bound linkers could move, at the cost of filament translational entropy. We suspect that Casimir interactions may drive a such transition from an aligned filament phase to a sliding phase as a function of filament length.

**Acknowledgments**

We would like to thank R. Bruinsma for helpful conversations. We acknowledge partial support from NSF-CMMI-1300514. K. Müller acknowledges the support by the Institute for Advanced Study (TUM-IAS) and the International Graduate School of Science and Engineering (IGSSE), TUM, Germany.

[1] C. J. Cyron, K. W. Müller, K. M. Schmoller, A. R. Bausch, W. A. Wall, and R. F. Bruinsma, Europhys. Lett. **102**, 38003 (2013).
[2] M. Gardel, J. Shin, F. MacKintosh, L. Mahadevan, P. Matsudaira, and D. Weitz, Science **304**, 1301 (2004).
[3] B. Wagner, R. Tharmann, I. Haase, M. Fischer, and A. R. Bausch, Proc. Natl. Acad. Sci. **103**, 13974 (2006).
[4] O. Pelletier, E. Pokidysheva, L. S. Hirst, N. Bouxsein, Y. Li, and C. R. Safinya, Phys. Rev. Lett. **91**, 148102 (2003).
[5] K. Schmoller, O. Lieleg, and A. Bausch, Biophys. J. **97**, 83 (2009).
[6] O. Lieleg, M. M. A. E. Claessens, C. Heussinger, E. Frey, and A. R. Bausch, Phys. Rev. Lett. **99**, 088102 (2007).
[7] D. Kachan, R. Bruinsma, and A. J. Levine, Phys. Rev. E **87**, 032719 (2013).
[8] L. van Hove, Physica **16** (1950).
[9] I. Langmuir, J. Am. Chem. Soc. **40**, 1361 (1918).
[10] H. B. G. Casimir, Proc. K. Ned. Adad. Wet. **51**, 793 (1948).
[11] B. Alberts, A. Johnson, J. Lewis, M. Raff, K. Roberts, and P. Walter, *Molecular biology of the cell* (Garland Science, 2002).
[12] M. E. Fisher, The Journal of Chemical Physics **45**, 1469 (1966), URL `http://scitation.aip.org/content/aip/journal/jcp/45/5/10.1063/1.1727787`.
[13] C. J. Cyron and W. A. Wall, Int. J. Numer. Meth. Engng **90**, 955 (2012).
[14] C. J. Cyron, K. W. Müller, A. R. Bausch, and W. A. Wall, J. Comput. Phys. **244**, 263 (2013).
[15] G. Jelenic and M. A. Crisfield, Computer Methods in Applied Mechanics and Engineering **171**, 141 (1999), ISSN 0045-7825, URL `http://www.sciencedirect.com/science/article/B6V29-3WJ7P5F-9/2/4cfc171b48fc4930b61cc3ef48fe8fdf`.
[16] M. A. Crisfield, *Non-linear Finite Element Analysis of Solids and Structures, Volume 2: Advanced Topics* (Wiley, Chichester, 2003).
[17] I. Romero, Computational Mechanics **34**, 121 (2004), URL `http://dx.doi.org/10.1007/s00466-004-0559-z`.
[18] J. Howard, *Mechanics of Motor Proteins and the Cytoskeleton* (Sinauer Associates, Sunderland, 2001).
[19] C. J. Cyron and W. A. Wall, Phys. Rev. E **80**, 066704 (2009), URL `http://link.aps.org/doi/10.1103/PhysRevE.80.066704`.
[20] C. J. Cyron and W. A. Wall, Phys Rev E **82**, 066705 (2010).
[21] E. H. Lieb and D. C. Mattis, *Mathematical Physics in One Dimension: Exactly Soluble Models of Interacting Particles, a Collection of Reprints with Introductory Text, by Elliott H. Lieb [and] Daniel C. Mattis* (Academic Press, 1966).
[22] L. Tonks, Phys. Rev. **50**, 955 (1936).
[23] D. Kachan and A. J. Levine (2017), unpublished.
[24] H. Shin, K. R. P. Drew, J. R. Bartles, G. C. L. Wong, and G. M. Grason, Phys. Rev. Lett. **103**, 238102 (2009).
[25] I. Borukhov, R. F. Bruinsma, W. M. Gelbart, and A. J. Liu, Phys. Rev. Lett. **86**, 2182 (2001), URL `http://link.aps.org/doi/10.1103/PhysRevLett.86.2182`.
[26] I. Borukhov, K.-C. Lee, R. F. Bruinsma, W. M. Gelbart, A. J. Liu, and M. J. Stevens, The Journal of Chemical Physics **117**, 462 (2002), URL `http://scitation.aip.org/content/aip/journal/jcp/117/1/10.1063/1.1481382`.
[27] K. W. Müller, R. F. Bruinsma, O. Lieleg, A. R. Bausch, W. A. Wall, and A. J. Levine, Phys. Rev. Lett. **112**, 238102 (2014).
[28] Since the dynamics of the filament is prescribed by a fourth-order differential equation, two consecutive cross linkers that each fix the position and slope set all the boundary conditions for that filament segment; the configuration of the neighboring segments does affect it. Thus, there is no interaction between next-nearest-neighbor linkers mediated by the fluctuations of the filament. Smaller values of $\alpha$ allow only some dynamical information to leak through linker sites, allowing for a subdominant next-nearest-neighbor interaction.